

PaperID AU196

Author Ravi Mishra , Essar Oil & Gas Exploration and Production Ltd. , India

Co-Authors Urmi Surve and Ashish Kumar

Pitfalls of High Amplitude Reflections from Shales in the Shelf-Margin, Mumbai Offshore Basin

Abstract

In conventional petroleum exploration, the contributors of seismic amplitude in shale section are very often overlooked and likely chances of getting misled by it in future exploration endeavors are high. In conventional shales, variation of elastic properties which cause seismic amplitude depends on mineralogy, compaction and texture. An attempt has been made to analyze the cause of seismic amplitudes in the shales of upper Miocene-recent of Chinchini formation at the Shelf Margin of Mumbai offshore basin. We resort to rock-physics depth trends of different facies (e.g. shales, calcareous shales, water and hydrocarbon saturated siltstones) to analyze and predict depth dependent AVO behavior. We find that interpretation of AVO-Inverted product stack i.e. Intercept*Gradient ($A*B$) volume supported by rock-physics modeling not only better disentangles the hydrocarbon saturated zones from the background (water saturated sandstone and shales) but also helps identify the cause of false seismic anomaly within the shale section itself. The efficacy of this technique is tested on two drilled locations with varying target depths at the study site.

Keywords: Shelf Margin, Conventional shales, Rock physics and AVO

Introduction

Till the end of 2015, Shelf-Margin did not record any significant hydrocarbon discovery. In the early 2016, an exploratory well A (drilled in the study area) made significant gas discovery (932-938m) from the clastic reservoir (a clean siltstone) of Pliocene within Chinchini formation as shown in Fig.1 (a) and Fig.1(c). This result encouraged to further probe a deeper target within the same Chinchini formation (upper Miocene) in another fault block for which Well B was planned as shown in Fig.1 (b) and Fig.1 (d). Seismic anomaly in Fig.1(d), a deeper target, at first glance looked very promising and similar to the one at the Pliocene discovery in Well A but drilling of this target resulted in encountering predominantly shales. Our attempt is to investigate the causative factor of misleading seismic anomaly at well B.

In the coming sections, the terms shales and calcareous shales will be used frequently. In the modeling, we assume that shales are made up of flakes of clay mineral and tiny fragment of silt-sized particle of other minerals especially quartz whereas calcareous shales are a mix of not only clay and quartz but also significant amount of calcite mineral. Shales and calcareous shales combined together are considered as conventional shales wherein TOC content ranges from less than 1.0% to 1.5% (Vernik, 2016, p.3). Shales normally constitute more than 80% of sediments and sedimentary rocks in siliciclastic environments. Shales are important both in controlling the overburden seismic wave propagation as well as the reflectivity contrast between cap rocks and reservoir rocks in prestack seismic data. Therefore, during AVO analysis it is crucial to understand the seismic properties of shales as a function of mineralogy and compaction (Avseth et al., 2008). In this study, we focus on:

1. rock physics modeling
2. depth trend analysis of shales, calcareous shales, water and hydrocarbon saturated siltstones
3. depth dependent product attribute ($A*B$) analysis and its application to seismic data

Finally it is demonstrated that product stack derived from seismic gather matches very well with the expected product attribute. It is also shown that false seismic anomaly can be avoided in shale using rock physics constrained interpretation during exploration.

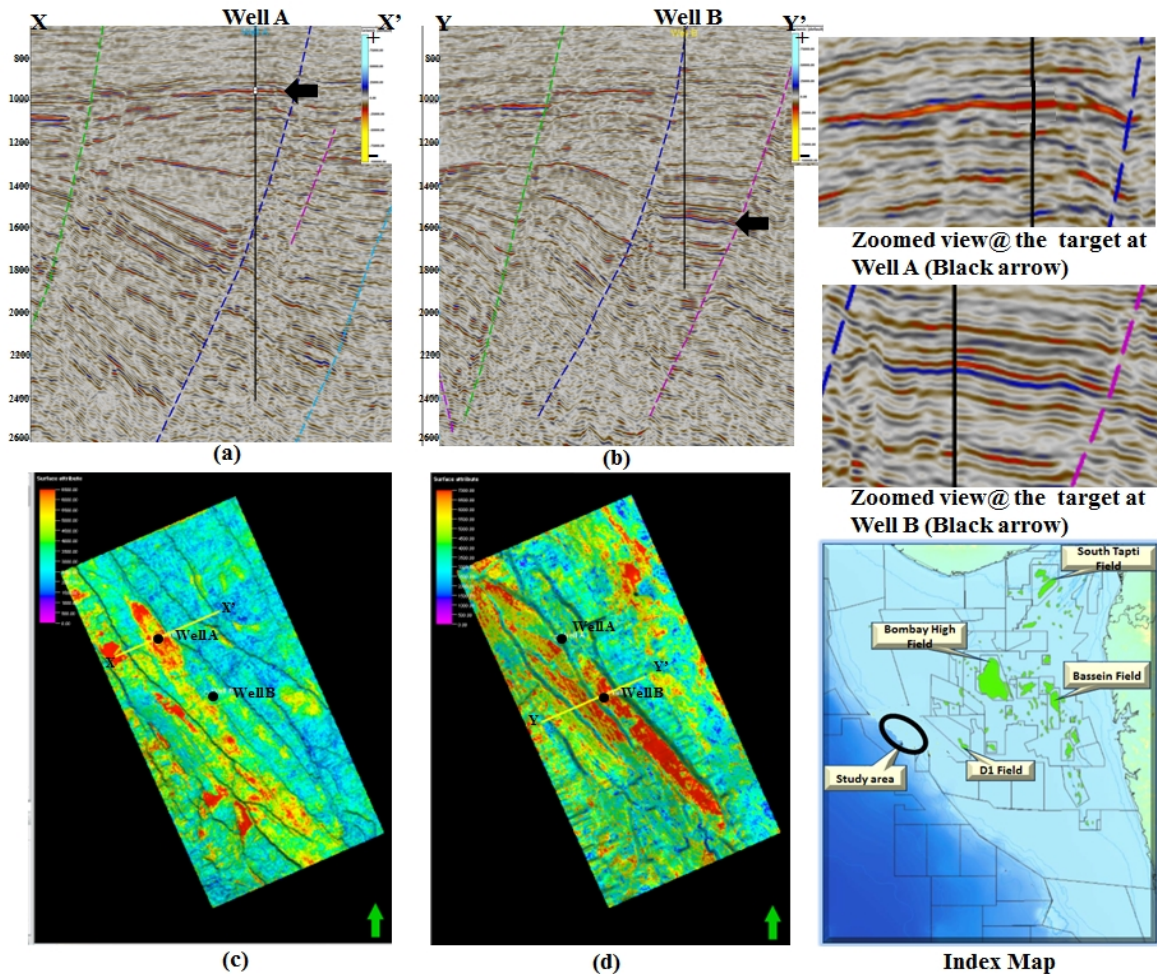


Fig.1.(a)Seismic dip line passing through well A (b) dip line passing through well B (c) RMS attribute extracted along the target in (a), (d) RMS attribute extracted along the target in (b).The targets are shown by arrow. Two zoomed seismic sections at the targets are also shown along with index map.

Rock physics modeling

Some of the most important breakthroughs in rock physics during the past decades have come not from additional mathematics, but from rediscovering the physics of rock geology (Avseth et al., 2005, p. xii). This holds true in our case too. For this study, we used two wells: Well A and Well B. Rock physics acts as a bridge between reservoir property porosity (ϕ) and elastic properties; P-wave velocity, S-wave velocity and bulk density (V_p , V_s and ρ_b). Effective pressure (i.e. confining pressure-pore pressure) and porosity trends shown in Fig.2(a) and Fig.2(b), which are the main inputs to the modeling were taken to be consistent with the effective pressure and porosities obtained from the wells.

Dominant lithologies encountered in well A were shales, calcareous shales, claystones, streaks of limestone and siltstones whereas in Well B, all aforementioned lithologies were encountered except siltstones. Limestones of significant thickness were also encountered shallower than 500m in both the wells but were not taken into consideration. Further, well A struck 6 m of gas (gas zone-1) at 915m and ~2m of gas at 565m (gas zone-2). Because of lack of full dataset above 500m and below 2500m, we selected the interval between 500m and 2500m. Elastic properties of Well B have been superimposed on well A to establish a single model that not only holds good in the study area but also expected to work in the nearby vicinity too. In order to model depth dependent elastic properties of siltstones (dominantly quartz), we used soft sand model (Dvorkin & Nur, 1996) for unconsolidated sands/siltstones in this geological setup followed by Gassmann (Gassmann, 1951) fluid substitution for oil and gas. Oil API and oil and gas saturation in the model were taken to be 35 deg. (regional data) and 50% respectively. Fluid properties were calculated using Batzle and Wang (Batzle and

Wang, 1992) equations based on available temperature, pressure and salinity. One can debate the applicability of this theory for shales, as it assumes an isotropic spherical pack of grains. However, using co-ordination number as a fitting parameter, this theory can be useful for shales (Avseth et al., 2016). Alternatively one can apply inclusion based model for shale depth trends (Avseth et al., 2008). Mineral fractions in the model were taken to be consistent with multi-mineral results from logs. Water saturated limestone streaks in the interval of study have also been inserted just to see their behavior with depth. Actually its velocity and bulk density should be greater than that of all the facies considered in the study but it is almost overlapped by the velocity and bulk density of the siltstones because of shaliness. Therefore, depth trend of siltstones can be fairly used for the water saturated shaly limestones streaks too. After this, rock physics depth trends of shales, calcareous shales, followed by water, oil and gas saturated siltstone in terms of V_p , V_s and ρ_b were generated. Depth trends after getting superimposed on the recorded logs fit agreeably with the facies encountered during drilling as shown in Fig.2(c), Fig.2(d) and Fig.2(e).

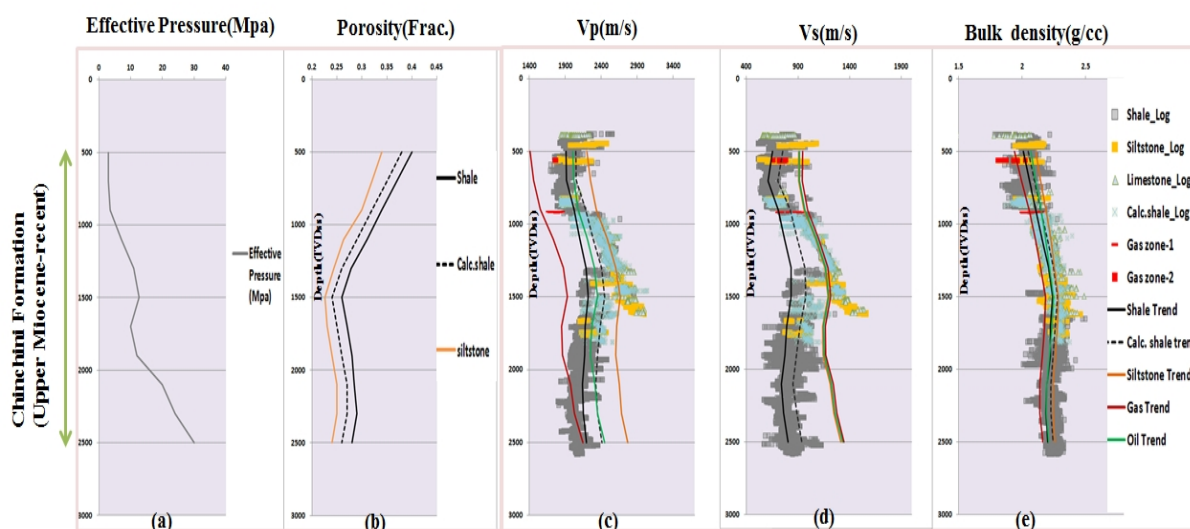


Fig.2 Rock physics depth trends (a) Effective pressure trend (b) porosity trends (c) V_p trends of shale (solid black), calcareous shale (dotted black), oil (solid green), water (solid orange) and gas (solid red) (d) superimposed on the recorded logs. V_s trends of shale, calcareous shale, oil, water and gas (e) bulk density trends of shale, calcareous shale, oil, water and gas. V_s trend being fluid independent, shows overlapping of water, oil and gas saturated siltstone trends as in Fig.(d).

P and S-impedance depth trends are also superimposed on the impedance logs shown in Fig.3(a) and Fig.3(b). Then AVO modeling was performed assuming two half spaces at each depth of interest taking parameters from rock physics trends at every 200m of interval. Three geological possibilities were assumed: 1) calcareous shales encased in shales 2) water and hydrocarbon siltstones encased in shales and 3) water and hydrocarbon siltstones encased in calcareous shales; but for display only four levels were chosen as shown in Fig.3(c). The expected AVO behavior of the siltstones saturated with water, oil and gas encased in shales and calcareous shales respectively at the depth of interests are shown in Fig.3(c). AVO modeling was carried out using three term Wiggins's formula (Wiggins et al., 1983). Finally depth trends of the product attribute Intercept*Gradient ($A*B$) from the respective V_p , V_s , and ρ_b trends were ready for the aforesaid geological possibilities to compare with product attribute derived from seismic gather shown in Fig.4(a), Fig.4(b), Fig.4(c), Fig.4(d) and Fig.4(e).

Rock physics depth trend analysis

Upper Miocene section in the Shelf Margin showed seismic amplitudes which at first glance appeared promising as in Fig.1 (d) but drilling resulted in only shales. In this section, the cause of the high amplitudes due to shales will be investigated by rock physics modeling and depth trend analysis. From 500m-900m, the effective pressure does not change considerably and from 900m-1500m, it gradually increases. Further, it starts decreasing below 1500m followed by slight increase from ~1800m onwards. As a consequence porosity faces first gradual decrease followed by increase, as shown in Fig.2(a) and Fig.2(b). P-impedance trend of calcareous shales is less than that of water

saturated siltstone and greater than that of shale trend, and follows the oil trend. This trend also shows a geological possibility at any depth between 500m--2500m when calcareous shale encased in shale will produce seismic reflection. The reflection may further be boosted by the tuning phenomenon if there is alteration of shale and calcareous shale. This was verified by the drilling results in well B wherein alterations of shale and calcareous shale were encountered. P-Impedance of gas trend is even less than that of shale which falls very close to discovered gas zone as shown in Fig.3(a). Gas trend does not match with gas zone-2 (shallower one) because a very clean siltstones were assumed in the model while the gas zone-2 had a bit shaly siltstone.

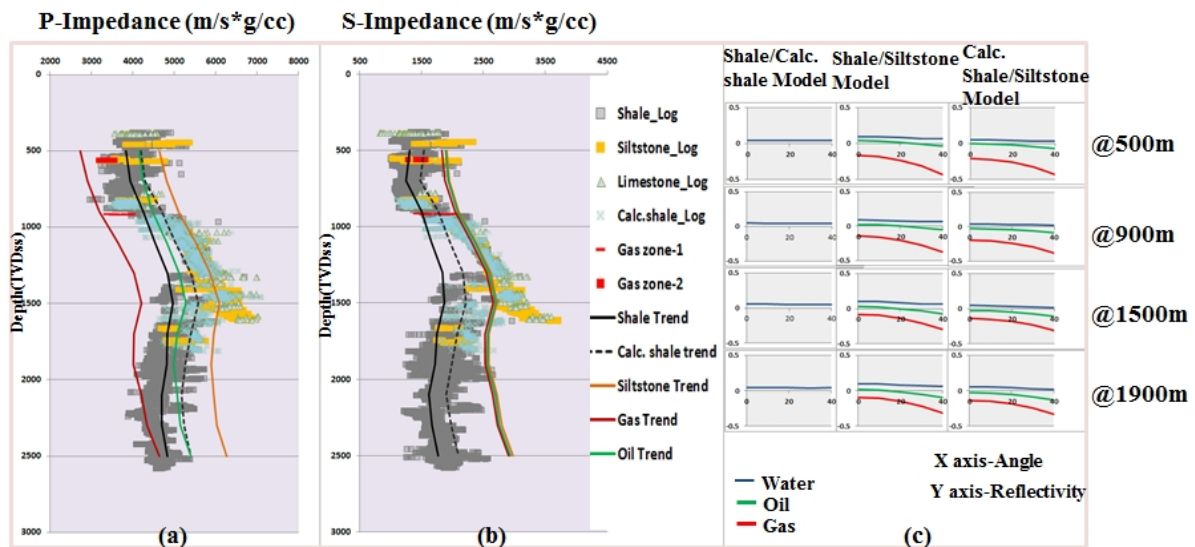


Fig.3 Rock physics depth trends (a) P-impedance trends of shale (solid black), calcareous shale (dotted black), oil (solid green), water (solid orange) and gas (solid red) superimposed on the recorded logs (b). S-impedance trends of shale, calcareous shale, oil, water and gas (c) depth dependent AVO first when calcareous shale encased in shale, second water and hydrocarbon siltstone encased in shale, and third water and hydrocarbon siltstone encased in calcareous shale. For display, only four levels were chosen. S-impedance trend being fluid independent, shows overlapping of water, oil and gas saturated siltstone trends as in (b).

It is observed that there is a gradual decrease specially in the V_s or S-impedance (a fluid independent property) of shale trend with depth from 500m to 900m, which can be explained as due to increase in the clay volume of the shales with no considerable change in effective pressure as shown in Fig.2(a) and Fig.3(b). It is also evident in Fig.3(b) that S-impedances of shales and calcareous shales start increasing suddenly between 900m-1500m deviating from normal trend. This can be explained as due to change in mineralogy of clay from montmorillonite to kaolinite (a heavier mineral) and gradual increase in effective pressure. Of course the siltstones too in the interval (900-1500m) are not devoid of clay and pressure independent. This in turn exhibits that not only shales and calcareous shales but siltstone too witness a stiffening effect as it can be observed in V_s or S-impedance trend. Change in mineralogy is also corroborated with multi-mineral study from logs. There does exist some uncertainty because of the lack of XRD study. However considering kaolinite as a clay mineral in the rock physics model along with gradual increase in effective pressure, a stiffening effect was observed and the depth trends showed good match with recorded logs. Beneath 1500m, lithology is mainly shales and calcareous shales intercalated alternatively and their respective mineral fractions do not vary considerably with depth. However, this interval does show a decrease in impedance and increase in porosity with depth as shown in Fig.2(b) and Fig.3(b). This can be explained as due to increase in pore pressure (i.e. decrease in effective pressure).

Product attribute (A*B) analysis and its application to real seismic

Depth dependent product attribute (A*B) was modeled by assuming; first when calcareous shales was encased in shales, second water and hydrocarbon siltstones encased in shales, and third water and hydrocarbon siltstones encased in calcareous shales as shown in Fig.4(a), Fig.4(b) and Fig.4(c). Polarity convention used in the study is the increase of acoustic impedance taken as peak (blue event in the seismic shown). It is observed that the product attribute shows large positive response (large -

ive intercept * large -ive gradient, Class III AVO) up to 2500m in case of gas saturated siltstone whether encased in shale or calcareous shale as shown in Fig.4(b) and Fig.4(c). Although the magnitude does decrease with compaction. Calcareous shale encased in shale results in seismic anomaly with small negative product response (slight +ive intercept * slight -ive gradient, AVO between Class I and Class IIP) and water saturated siltstone too encased in shale or calcareous shale shows a small negative product response (slight +ive intercept * slight -ive gradient, AVO between Class I and Class IIP) in the entire interval of the study.

As far as oil driven AVO product is concerned, it exhibits slight negative product response (slight -ive intercept * slight +ive gradient, AVO range from Class IIP-Class II) in the entire interval of the study when encased in shale but slight positive product response (slight -ive intercept * slight -ive gradient, AVO range from Class IIP-Class II) between 800m-2000m when encased in calcareous shale as shown in Fig.4(c). However, oil driven response in both the cases of encasing media falls very close to the water driven response. Further, this slight positive response of oil is not at all comparable to the gas driven response. This non uniqueness of oil with water saturated zones, can be explained by petroleum system modeling (PSM). In this case, PSM showed that the primary and proven source rock which is Panna formation (Eocene) has gone in dry gas window and other shales of Oligocene do not have sufficient TOC to generate oil. Therefore, chances of finding oil with slight negative or slight positive product response may be ruled out. This result was extended to the product stack derived from seismic gather and it was found that the expected positive product response matched nicely with the product stack in the gas zone 1 (blue event as +ive response in well A shown by arrow in Fig.4(d)) and no gas zone in well B (red event as -ive response, shown by arrow in Fig.4(e)). As at target level in well B, the lithologies encountered were calcareous shale intercalated with shale. This demonstrates that the AVO product model is working convincingly on the two selected locations and is expected to work in nearby area too.

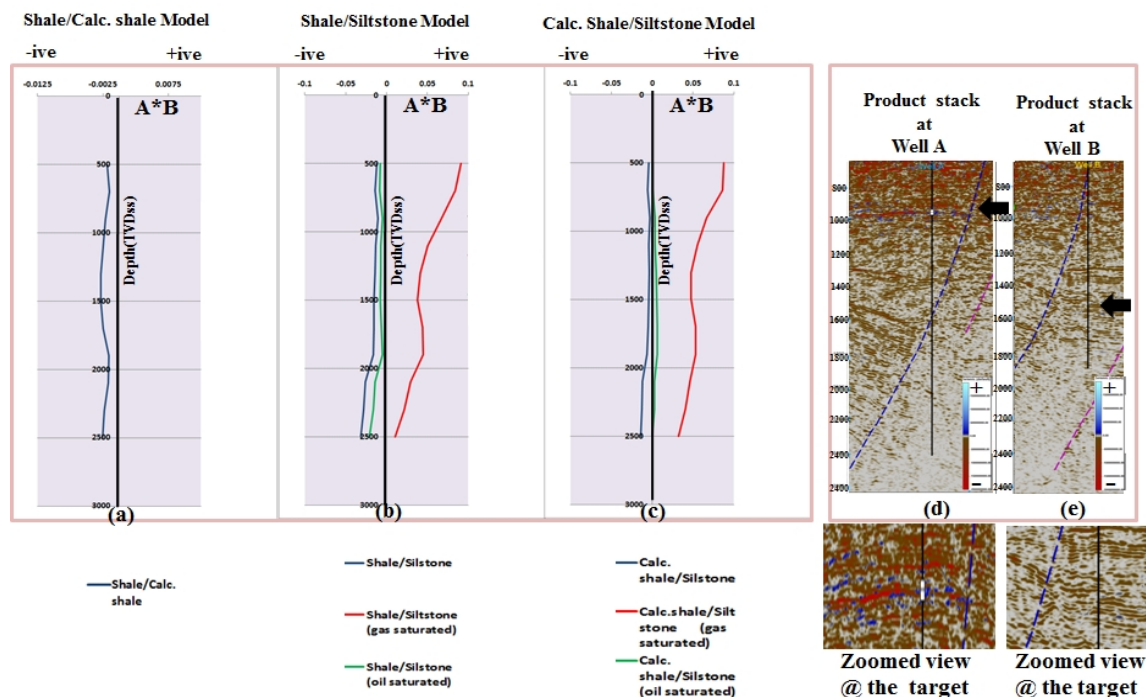


Fig.4 showing depth dependent AVO behavior (product attribute) for the three geologic possibilities: first when calcareous shale encased in shale, second water and hydrocarbon siltstone encased in shale, and third water and hydrocarbon siltstone encased in calcareous shale as shown in Fig.(a), Fig.(b) and Fig.(c). Fig.(d) and Fig.(e) show seismic gather derived product attribute at well A and well B along with their zoomed view at the targets shown by black arrows. In the zoomed product stack the amplitude in blue (gas zone) shows positive response in well A and red negative response where non reservoir i.e. calcareous shales intercalated with shales were found. Seismic sections (time domain) of the product attribute derived from pre-stack seismic data have been adjusted with the modeled product attribute (depth domain) by velocity.

Conclusion

Effects of many competing factors which may produce similar seismic reflections in the subsurface, can be correctly deduced by rock physics constrained interpretation. This helps to understand the cause of seismic reflections not only from reservoir zones but also from the non-reservoirs (conventional shales in our case). This study shows that from 500m to 900m, minerals are the dominant contributors of seismic events. From 900m to 1500m seismic events are affected by both the change in clay mineralogy from montmorillonite to kaolinite and effective pressure. Below 1500m seismic events are affected dominantly by the increase in pore pressure. Calcareous shale encased in shale results in seismic anomaly with small negative product response at all depths. Gas saturated siltstone encased in shale or calcareous shale shows large positive product response whereas water saturated siltstone in both the cases of the encasing media shows a negative product response in the entire interval of the study. As far as oil driven product is concerned, it exhibits slight negative product response when encased in shale at all depth and slight positive product response between 800m-2000m when encased in calcareous shale. However, in both the cases, oil driven response falls very close to water. This non uniqueness of oil with water saturated zones can be deduced if it is integrated with petroleum system modeling. Finally the product attribute delivers convincing results on both the selected locations (well A and well B). Rock physics modeling reveals that under compacted to moderately compacted reservoir facies (siltstones) and non-reservoir facies (shales and calcareous shales) are present in the study area. It is suggested that seismic anomaly can be targeted for gas only if it shows positive product value (Class III AVO). Further, the study can be extended to other blocks in the Shelf Margin of the Mumbai offshore basin if target lies within the Chinchini formation.

Acknowledgement

The authors are thankful to Essar Oil & Gas and Exploration and Production Ltd. (EOGEPL) to publish this paper and special thanks to Mr. D. Pavithran (DGM-Geology, EOGEPL) for throwing light on drilling related discussions.

References

- Avseth, P., Mukherji, T., and Mavko, G., 2005, Quantitative seismic interpretation-Applying rock physics tools to reduce interpretation risk: Cambridge University press.
- Avseth, P., Draege, Anders, Johansen, T., JØrstad, A., 2008, Shale rock physics and implications for AVO analysis: A North Sea demonstration, The Leading Edge.
- Avseth, P., and Lehoccki, I., 2016, Combining burial history and rock physics modeling to constrain AVO analysis during exploration.
- Batzle, M., and Wang, Z., 1992, Seismic properties of pore fluids, Geophysics, vol.,57, No.11(Nov.1992), P. 1396-1408.
- Dvorkin, J. and Nur, A., 1996 Elasticity of high porosity sandstones: Theory for two North sea datasets, Geophysics, 61, 1363-1370, doi;10.1190/1.2172312.
- Gassmann, F., 1951, Elasticity of porous media: Uber die Elastizitat poroser Medien: Vierteljahrsschrift der Naturforschenden Gesselschaft , 96, 1-23.
- Vernik, L., 2016, Seismic Petrophysics in quantitative interpretation: Society of Exploration Geophysicists.
- Wiggins, R., Kenny, G. S., and McClure, C. D., 1983, A method for determining and displaying the shear velocity reflectivities of a geologic formation. European Patent Application 0113944.